

Static and Dynamic Autonomic Response with Increasing Nausea Perception

LAUREN T. LACOUNT, RICCARDO BARBIERI, KYUNGMO PARK,
JIEUN KIM, EMERY N. BROWN, BRADEN KUO,
AND VITALY NAPADOW

LACOUNT LT, BARBIERI R, PARK K, KIM J, BROWN EN, KUO B, NAPADOW V. *Static and dynamic autonomic response with increasing nausea perception*. *Aviat Space Environ Med* 2011; 82:424-33.

Background: Nausea is a commonly occurring symptom typified by epigastric discomfort with urge to vomit. The relationship between autonomic nervous system (ANS) outflow and increasing nausea perception is not fully understood. **Methods:** Our study employed a nauseogenic visual stimulus (horizontally translating stripes) while 17 female subjects freely rated transitions in nausea level and autonomic outflow was measured (heart rate, HR; heart rate variability, HRV; skin conductance response, SCR; respiratory rate). We also adopted a recent approach to continuous high-frequency (HF) HRV estimation to evaluate dynamic cardiovagal modulation. **Results:** HR increased from baseline for all increasing nausea transitions, especially transition to strong nausea (15.0 ± 11.4 bpm), but decreased (-6.6 ± 4.6 bpm) once the visual stimulus ceased. SCR also increased for all increasing nausea transitions, especially transition to strong nausea (1.76 ± 1.68 μ S), but continued to increase (0.52 ± 0.65 μ S) once visual stimulation ceased. LF/HF HRV increased following transition to moderate (1.54 ± 2.11 a.u.) and strong (2.57 ± 3.49 a.u.) nausea, suggesting a sympathetic shift in sympathovagal balance. However, dynamic HF HRV suggested that bursts of cardiovagal modulation precede transitions to higher nausea, perhaps influencing subjects to rate higher levels of nausea. No significant change in respiration rate was found. **Conclusions:** Our results suggest that increasing nausea perception is associated with both increased sympathetic and decreased parasympathetic ANS modulation. These findings corroborate past ANS studies of nausea, applying perception-linked analyses and dynamic estimation of cardiovagal modulation in response to nausea.

Keywords: motion sickness, heart rate variability, skin conductance response, galvanic skin response, vestibular.

NAUSEA IS A COMMONLY occurring symptom typified by epigastric discomfort with the urge to vomit. It can arise from a variety of causes, including as a side effect of pharmacotherapy and general anesthesia, as a side effect of fluctuating hormone levels during pregnancy, and as a consequence of visual/vestibular sensory discordance. This latter cause, termed motion sickness, typifies the root of the word "nausea" (derived from "naus" or "ship" in Greek), and has been commonly adopted in experimental settings to study physiological responses to nausea (24).

Motion sickness is a conglomeration of individual symptoms, which can be grouped by factor analysis (19). One factor is specifically related to nausea and includes the following symptoms: stomach awareness, burping, increased salivation, sweating, and nausea. However, other factors include oculomotor (e.g., eye strain, blurred vision) and disorientation (e.g., dizziness)

symptoms, which are all concomitant with nausea during motion sickness. Severity or even occurrence of motion sickness varies appreciably among individuals, and motion sickness symptoms and susceptibility have a complex relationship with ethnicity and gender. For instance, individuals of Asian descent tend to be more susceptible to motion sickness than Caucasian individuals (22,24) and responses to motion sickness susceptibility questionnaires have been found to differ between men and women (22).

The underlying mechanism of motion sickness is postulated to be a conflict between the visual and vestibular systems, but can also occur due to conflict within the vestibular (34) and visual (20) systems themselves. Hence experimental induction of motion sickness has appropriated rotating chairs (11,13,16,18,30,37), virtual reality or simulator systems (21,28), or optokinetic drums (8), in which the subject remains stationary and a striped drum rotates around their head. Ultimately, motion sickness is known to be strongly influenced by the autonomic nervous system (ANS) (17,31) as well as the vestibular (17), cognitive (24), and neuroendocrine systems (17).

ANS response to nausea spans multiple end organs and includes both sympathetic and parasympathetic outflow. Prior studies have measured a variety of autonomic physiological variables and have generally found that motion sickness increases both heart rate (10,21,28,37) and skin conductance (10,18,21), a measure of sympathetic output to sudomotor glands in the skin (17). More precise cardio-autonomic modulation has been estimated by measures of heart rate variability (HRV). With this analysis approach, spectral analysis assesses sympathovagal modulation by measuring the magnitude of a high-frequency (influenced by cardiovagal outflow)

From the Martinos Center for Biomedical Imaging, Department of Radiology, Massachusetts General Hospital, Charlestown, MA.

This manuscript was received for review in September 2010. It was accepted for publication in November 2010.

Address correspondence and reprint requests to: Vitaly Napadow, Ph.D., Martinos Center for Biomedical Imaging, Department of Radiology, 149 Thirteenth St., #2301, Charlestown, MA 02129; vitaly@nmr.mgh.harvard.edu.

Reprint & Copyright © by the Aerospace Medical Association, Alexandria, VA.

DOI: 10.3357/ASEM.2932.2011

and low-frequency (both sympathetic and parasympathetic) peak in the heart rate power spectrum (26). High-frequency (HF) HRV has been found to decrease during motion sickness (13) in one study, increase during another (21), and remain unchanged in a third (30). This inconsistency may have been due to variability in stimulus intensity [stemming from the form of motion sickness stimulus used (20), i.e., visual only (21) versus actual physical rotation (13,30)] as well as measurement and analysis techniques (13,21,30).

In this study, we aimed to address inconsistencies in past studies and apply recent adaptive point-process algorithms for estimating dynamic HRV response to illusory motion induced nausea. We applied an experimental design wherein a visual display of translating stripes encompasses the entire field of view for supine individuals previously deemed susceptible to motion sickness. Skin conductance, electrocardiography, and respiration were all monitored in order to assess various ANS response metrics in conjunction with subjective naturalistic reports of worsening nausea. We hypothesized that increasing nausea would elicit increasing sympathetic modulation, while dynamic trends in HF HRV would demonstrate characteristic fluctuations of parasympathetic (cardiovascular) modulation both prior and following subjective transitions to increasing nausea.

METHODS

Subjects

Participants included female, right-handed [Edinburgh Inventory (33)] subjects with a mean age of 28.4 yr (SD = 8.5 yr) and increased susceptibility to motion sickness, as indicated by a score greater than 60 on the Motion Sickness Susceptibility Questionnaire (MSSQ) (15). A MSSQ level of 60 was chosen because it represented a visible inflection point in the graph provided by the study developing this instrument. Thus, subjects with MSSQ scores higher than 60 reliably reached moderate nausea perception and did so faster than those with lower scores (15). Subjects were instructed to abstain from food and water for 12 h, and from cigarettes and alcohol for 24 h, prior to the experiment. This was deemed necessary for safety reasons, as subjects would be stimulated to the verge of vomiting. All experiments took place between 0700 and 1200 at the Martinos Center for Biomedical Imaging in Boston, MA. Informed consent was obtained from all participants, and the protocol was approved by the Human Research Committee of Massachusetts General Hospital.

There were 30 motion sickness prone subjects who underwent a training session, with 21 experiencing high enough nausea that they were asked to continue on to the next experimental session, which was performed inside an MRI scanner. Of the 21 subjects who completed the experimental session, 3 were not included in our analyses because their maximum nausea rating was a "2" ("moderate" nausea). This was done to limit heterogeneity in the subjects, such that all subjects included in the analysis reached at least a "strong," if not "severe"

level of nausea. Another subject was not included because her pre-experiment (baseline) nausea level started at a "2," while all other subjects began at "0." Thus, 17 subjects were ultimately included in the analysis. Due to MRI scanner noise, the ECG could not be annotated for one subject, who was thus excluded from heart rate (HR) and HRV analyses, while three other subjects had poor respiratory data quality and were excluded from those analyses.

Procedure

The study was divided into two sessions. During the first (training) session, subjects were familiarized with the experimental setup and nauseogenic stimulus. If subjects attained a sufficiently high level of nausea and if they chose to remain in the study, they returned (at least 12 d later) to a second experimental session. The physiological data presented here were collected as part of this second, more controlled, experimental session that also included functional MRI (fMRI) data acquisition. This fMRI data will be presented in a future publication as they are outside the scope of this ANS-focused analysis.

Subjects were placed, supine, in a 1.5T Siemens Avanto MRI scanner (Siemens Medical Systems, Erlangen, Germany). A specialized 23-channel head coil constructed at the Martinos Center for Biomedical Imaging (38) was used to allow for unimpeded visual stimulation. A concave screen was positioned 10 cm in front of their eyes, onto which visual stimuli were projected from behind. The head of the subject was immobilized in the MRI head coil, with cushions on either side, thereby insuring no head tilt maneuvers (Fig. 1A), which are known to strongly influence visual stimulus induced motion sickness via pseudo-Coriolis effects (6). Importantly, the concave screen comprised the entire field-of-view (150°) of the subject. The visual stimulus procedure for both sessions was divided into three different (but contiguous) periods (Fig. 1B). The first and last periods were each 5 min in length, during which subjects were asked to lie still and stare directly ahead at a cross hair projected onto the center of the screen. Between these two periods, subjects were presented with a nauseogenic visual stimulus of black/white stripes (black stripes 1.2 cm, 6.9° viewing angle; white stripes 1.85 cm, 10.6° viewing angle) translating left-to-right at an apparent speed of $62.5^\circ \cdot s^{-1}$. This left-to-right horizontal translation induces a linear vection sensation wherein subjects experience a false sensation of translating to the left (20,24). Similar full field-of-view vection stimuli in supine subjects have successfully been used in the past (9). The maximum duration of our nauseogenic stimulus was 20 min, but was shortened in some subjects based on these subjects reaching a predetermined maximum level of discomfort. Subjects were instructed to maintain a constant, natural, respiratory rate throughout the experiment to improve HRV interpretability (4,26) and to prevent self-inhibition of increasing nausea (1,12). Subjects were also asked to keep their eyes open and just let the nausea sensation evolve, knowing that a rating of severe nausea will terminate the stimulus. These instructions

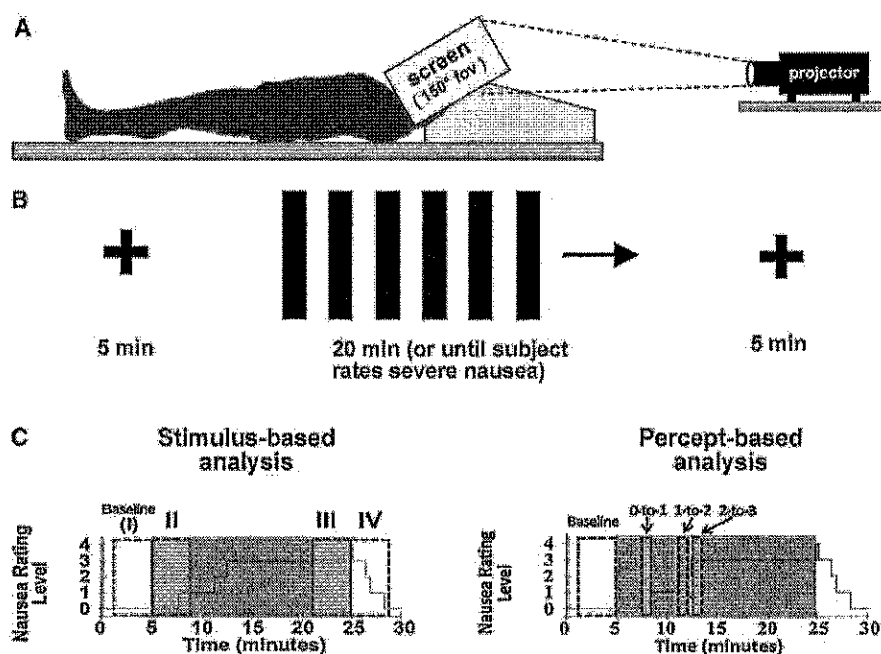


Fig. 1. Experimental procedure and analysis approach. A) Subjects lay supine while a nauseogenic visual stimulation (horizontally translating stripes) was projected onto a full field-of-view screen from behind. B) The visual stimulus was comprised by cross-hair fixation for 5 min before and after linear vection stimulus, which lasted up to 20 min, or until the subject rated a nausea level "4" for "severe" nausea. C) Autonomic data were analyzed with both a stimulus-based (left) and perception-based (right) approach, where data averaged over discrete windows were compared to data collected during cross-hair fixation at baseline.

were described before and after the training session in order to give subjects feedback and practice in limiting self-inhibition. Instructions were again repeated just prior to the experimental session.

Subjects were instructed to rate their level of nausea using an intensity scale of "0" to "4." These ratings were practiced during the training session, to better familiarize subjects with rating nausea intensity. Subjects were instructed that a rating of "4" indicated "severe" nausea, where subjects felt they were on the verge of vomiting from their past experience. A rating of "3" indicated "strong" nausea, a rating of "2" "moderate" nausea, a rating of "1" indicated "mild" nausea, and a rating of "0" indicated no nausea. Subjects knew that once they rated "4" for severe nausea, the stimulus would be terminated. During the experimental session, subjects were trained to use a 5-button button box to freely (not cued) rate their overall nausea level ranging from "0" to "4."

Following the experiment, subjects completed the Simulator Sickness Questionnaire (SSQ) (19) to report the severity of different motion sickness symptoms at each global (0-4) nausea level. As previously mentioned, motion sickness symptoms presented in the SSQ can be grouped into three factors: 1) nausea, 2) oculomotor, and 3) disorientation (19). A SSQ factor score was thus calculated for each global nausea level for each subject. We then used repeated-measures ANOVA to test for significant differences in factor score among these global nausea levels, followed by post hoc paired *t*-tests to determine which global levels were significantly different from one another for each SSQ factor.

Equipment and Single Subject Analysis

All physiological signals were collected at 400 Hz using Chart Data Acquisition Software (ADInstruments, Colorado Springs, CO) on a laptop equipped with a 16-channel Powerlab DAQ System (ADInstruments). Physiological metrics were calculated within discrete windows of time using in-house developed tools (Matlab v. 7.1, The MathWorks, Inc., Natick, MA).

Skin conductance response (SCR): During the experiment, skin conductance level (SCL) was measured with Ag/AgCl finger electrodes (MLT117F, ADInstruments) attached to the palmar aspect of the second and fourth fingers of the nondominant left hand. A 10-Hz low pass filter was applied to the skin conductance signal. Mean SCL was calculated for discrete windows and compared to baseline according to the analysis procedures below.

Heart rate: An MRI-compatible Patient Monitor (Model 3150, InVivo Research, Inc., Orlando, FL) was used to collect subjects' electrocardiogram (ECG) signal through MRI-compatible electrodes (VerMed, Bellows Falls, VT) on the chest. Due to the existence of gradient switching artifact from the MRI scanner, HR and R-R interval obtained from ECG data were first annotated using automated methods [WaveForm DataBase Software Package (14)] followed by manual adjustments (Matlab v. 7.1, The MathWorks, Inc.) to assure correct QRS peak detection. Within each window of interest, the average heart rate was calculated. Due to MRI scanner noise, the ECG could not be annotated for one subject, who was thus excluded from HR and HRV analyses.

Heart rate variability: HRV was calculated from the same ECG signal used to calculate heart rate above. HRV for discrete time windows was calculated from the power spectral density of heart rate (resampled at 4 Hz from the inverted R-R interval time series) using in-house tools (Matlab v. 7.1, The MathWorks, Inc.). Calculations were performed for 4-min windows. The low-frequency power (LF) within each window was computed by taking the integral of the power spectrum between 0.04 and 0.15 Hz, while the HF power was computed as the integral between 0.15 and 0.4 Hz. Normalized LF power and normalized high-frequency power were evaluated by dividing LF and HF, respectively, by the integral of the power spectrum above 0.04. The ratio of LF to HF was also calculated following standard recommendations (26).

In addition, a novel adaptive recursive algorithm was applied to the R-R series to compute instantaneous estimates of HR and HRV from electrocardiogram recordings of R-wave events, i.e., "dynamic HRV." This approach is based on the point process methods already used to develop both local likelihood (2) and adaptive (3) heart rate estimation algorithms. This novel assessment of HRV has also been applied successfully in conjunction with fMRI recordings to characterize the brain correlates of cardiovagal modulation (32). The stochastic structure in R-R intervals is modeled as an inverse Gaussian renewal process. The inverse Gaussian probability density is derived directly from an elementary, physiologically based integrate-and-fire model (2,3).

We assume that given any R-wave event u_n , the waiting time until the next R-wave event, or equivalently, the length of the next R-R interval, obeys an inverse Gaussian probability density $f(t | u_n, \theta)$ where $t > u_n$. The model is defined, at any time t , as:

$$f(t | H_{u_k}, \theta) = \left[\frac{\theta_{p+1}}{2\pi(t - u_k)^3} \right]^{\frac{1}{2}} \exp \left\{ -\frac{1}{2} \frac{\theta_{p+1} [t - u_k - \mu(H_{u_k}, \theta)]^2}{\mu(H_{u_k}, \theta)^2 (t - u_k)} \right\} \quad \text{Eq. 1}$$

where $H_{u_k} = \{u_k, w_k, w_{k-1}, \dots, w_{k-p+1}\}$, $w_k = u_k - u_{k-1}$ is the k^{th} R-R interval, $\mu(H_{u_k}, \theta) = \theta_0 + \sum_{j=1}^p \theta_j w_{k-j+1} > 0$ is the mean, $\theta_{p+1} > 0$ is the scale parameter, and $\theta = (\theta_0, \theta_1, \dots, \theta_{p+1})$.

The model also represents the dependence of the R-R interval length on the recent history of parasympathetic and sympathetic inputs to the sinoatrial (SA) node by modeling the mean as a linear function of the last p R-R intervals. This set of p coefficients allows for decomposition of the spectral power (HRV) into the classic spectral components noted above: LF and HF (27).

The point process recursive algorithm is able to estimate the dynamics of the model parameters and, consequently, the time-varying behavior of each spectral index at any time resolution. This statistical model for deriving the HRV time series has been cross-validated with standard time-frequency domain approaches for

HRV analysis (2). The dynamic response for the point process method was found to provide a significant improvement in tracking fast dynamic changes when compared to the more conventional recursive least squares (RLS) algorithm (3). A fixed order $P = 8$ was chosen for the current analysis. Indices were updated every 10 ms and then resampled at 2 Hz.

For all subjects, Dynamic (point-process) HF HRV data were analyzed over five different 90-s temporal windows from 30 s before a "transition" to 60 s after that transition. For each subject, these "transitions" included the onset of the linear vection stimulus, "START"; rating increase from a level of 0 to a level of 1, "0-to-1"; increase to a rating level of 2, "1-to-2"; increase to a rating level of 3, "2-to-3"; and termination of the linear vection stimulus, "END." For consistency, the END window was only analyzed for subjects ($N = 12$) whose stimulus was terminated after they rated 4 (some subjects, $N = 5$, only reached a level 3). In order to average across subjects, these data were variance normalized by subtracting the mean and dividing by the SD.

Respiration: Respiration rate was calculated using the end tidal CO_2 (et CO_2) level collected via nasal cannula (Salter Labs, Arvin, CA) and the MRI-compatible Patient Monitor noted above. Average respiratory rate was estimated as the frequency of peak power of the discrete Fourier transform of the et CO_2 signal within each window of interest. Three subjects had poor respiratory data quality due to equipment failure and were excluded from analyses.

Group Data Analysis and Statistics

As subjects freely rated evolving nausea, analysis of SCR, HR, static HRV, and respiratory rate was performed through both stimulus- and perception-based approaches (Fig. 1C). The former was necessary to capture ANS response following vection stimulus termination, while the latter was necessary as different subjects rated nausea level transitions at different times during the experiment. For both approaches, the 4-min period immediately preceding the beginning of the nausea stimulus ("I" or "baseline") was used as a comparator baseline.

In the stimulus-based approach, which did not explicitly respect subject ratings, 4-min windows were taken immediately after the onset of the stimulus ("II") to reflect initial response, during the last 4 min of the stimulus ("III") when the subjects were the most nauseous, and during the 4 min immediately following the end of the stimulus ("IV") as the subjects recovered. A window length of 4 min was chosen to balance potential nonstationarity within the window with the need for adequate data vector size for HRV analyses.

In the perception-based approach, 1-min windows beginning at nausea level transitions (e.g., "1" to "2," or "2" to "3") were compared to the baseline level and to one another in order to determine ANS response to increasing perception of nausea symptoms. If subjects had more than one increasing nausea level transition (due to nausea level fluctuation), only the first such transition was used in order to limit heterogeneity.

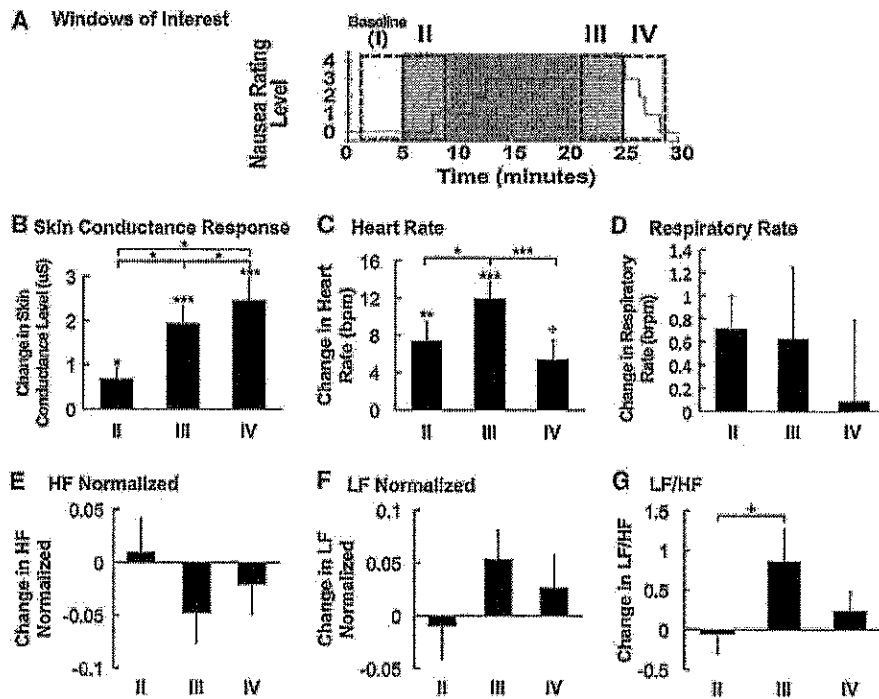


Fig. 2. Stimulus-based analysis of physiological indices. A) Timing of 4-min windows of interest are shown over a plot of a representative subject's nausea level. B-C) Average change in skin conductance, HR, respiratory rate, normalized HF, normalized LF, and LF/HF ratio in response to increasing duration of nausea stimulus. Error bars indicate standard error of the mean. + $0.1 > P > 0.05$, * $0.05 > P > 0.01$, ** $0.01 > P > 0.001$, *** $P < 0.001$.

For both analysis methods, physiological measures were compared with each other and with baseline in two steps. We first used a repeated measures analysis of variance (ANOVA) to test for significant differences among the windows of interest, followed by post hoc paired *t*-tests to determine which windows were significantly different from one another. As there were multiple post hoc tests covering multiple windows of interest, a Bonferroni correction was applied to correct for multiple comparisons. Significance was set at $P = 0.05$, with $0.1 > P > 0.05$ considered trending values (SPSS for Windows v. 10.0.7, SPSS, Inc., Chicago, IL).

An example of evolving nausea rating, SCL, HR, point process HF power, and respiratory rate from one subject over the course of the experiment are presented in a Fig. A online*.

RESULTS

Of the 17 subjects enrolled in this analysis (rating at least a "3" out of "4"), 12 subjects experienced nausea rated as "4," severe. The average duration of linear vection stimulus for those 12 subjects whose maximum nausea rating was "4" (and therefore terminated prior to the maximum 20 min) was 9.1 ± 4.5 min (mean \pm SD). For other intermediate nausea level transitions for all 17 subjects, the average duration until subjects reached the 0-to-1 transition was 1.9 ± 2.1 min, the 1-to-2 transition

was 3.8 ± 2.3 min, and the 2-to-3 transition was 6.9 ± 4.3 min. Of the 17 subjects, 9 monotonically increased their nausea ratings without any decreasing nausea level transitions. Eight subjects exhibited at least one decreasing level transition at some point during the experiment, which is not uncommon in linear vection studies where nausea sensation is known to fluctuate. This "drop-off" may have been due to spontaneous change in gaze focus and/or attention processes.

Of the 12 subjects who reached a global nausea level of 4, 9 subjects completed the SSQ. An initial repeated measures ANOVA indicated that there were differences in SSQ nausea factor intensity between the different global (0-4) nausea levels for the nausea specific factor [$F(3,24) = 119.4, P < 0.001$], oculomotor factor [$F(1,3,10.4) = 37.1, P < 0.001$, using Greenhouse-Geisser correction for Mauchly's *W* of 0.01 indicating nonsphericity], and disorientation factor [$F(3,24) = 86.7, P < 0.001$]. Post hoc testing demonstrated that all three symptom factors (nausea, oculomotor, and disorientation) increased in severity with increasing global nausea level ratings ($P < 0.01$ for all comparisons).

For the stimulus-based analysis, four 4-min temporal windows (immediately before and after both the onset and termination of the nauseogenic stimulus: "I," "II," "III," and "IV") were compared (Fig. 2A), revealing increases in SCR, HR, and LF/HF HRV over the course of the experiment. An initial repeated measures ANOVA indicated that there were within-subject differences among stimulus-based windows for average SCR [$F(1,3,20.8) = 15.7$,

* Online figures can be accessed via the "Online Journal" link at www.asma.org/journal/online_journal.php.

$P < 0.001$, using Greenhouse-Geisser correction for Maulchy's W of 0.04] (Fig. 2B), HR [F(3,45) = 16.7, $P < 0.001$] (Fig. 2C), and the ratio of LF to HF [F(3,45) = 3.5, $P = 0.02$] (Fig. 2G), but not for respiratory rate [F(3,39) = 0.6, $P = 0.6$], normalized HF [F(3,45) = 1.9, $P = 0.1$], or normalized LF [F(3,45) = 1.9, $P = 1$] (Figs. 2D, 2E, and 2F, respectively).

For the post hoc analyses, average SCL significantly increased over baseline for windows II, III, and IV [II: $\Delta = 0.68 \pm 0.98 \mu\text{S}$ (mean \pm SD), $P < 0.05$; III: $1.94 \pm 1.65 \mu\text{S}$, $P < 0.001$; IV: $2.46 \pm 2.11 \mu\text{S}$, $P < 0.001$] (Fig. 2B, Table I). SCL also increased over the course of the experiment (II to III: $\Delta = 1.26 \pm 1.71 \mu\text{S}$, $P < 0.05$; II to IV: $\Delta = 1.78 \pm 2.25 \mu\text{S}$, $P < 0.05$; III to IV: $\Delta = 0.52 \pm 0.65 \mu\text{S}$, $P < 0.05$) (Fig. 2B).

HR increased significantly over baseline for window II ($\Delta = 7.4 \pm 8.2$ beats per minute (bpm), $P < 0.01$); III ($\Delta = 12.0 \pm 7.0$ bpm, $P < 0.001$) and had a trending increase over baseline for window IV ($\Delta = 5.4 \pm 8.1$ bpm, $P = 0.05$) (Fig. 2C, Table II). Average HR increased significantly from II to III ($\Delta = 4.6 \pm 6.1$ bpm, $P < 0.05$), but decreased significantly from III to IV ($\Delta = -6.6 \pm 4.6$ bpm, $P < 0.001$) after the stimulus terminated (Fig. 2C). In regard to HRV, the ratio of LF to HF trended upward ($\Delta = 0.92 \pm 1.52$ a.u., $P = 0.08$) between windows II and III (Fig. 2G). No other significant differences or trends were found.

For the perception-based analysis approach, we compared 1-min temporal windows beginning just after state transition with baseline values (Fig. 3A). Overall, we found increases in SCR, HR, normalized LF, and LF/HF, and a decrease in normalized HF. An initial repeated measures ANOVA indicated significant differences among perception-based analysis windows for SCR [F(3,48) = 13.7, $P < 0.001$] (Fig. 3B), HR [F(3,45) = 18.4, $P < 0.001$] (Fig. 3C), normalized HF [F(3,45) = 3.6, $P = 0.02$] (Fig. 3E), normalized LF [F(3,45) = 4.0, $P = 0.01$] (Fig. 3F), and the ratio of LF to HF [F(3,45) = 5.7, $P < 0.01$] (Fig. 3G), but not respiratory rate [F(3,39) = 0.5, $P = 0.7$] (Fig. 3D).

In the post hoc analyses, SCR increased for 0-to-1 ($\Delta = 0.99 \pm 1.26 \mu\text{S}$, $P < 0.05$), for 1-to-2 ($\Delta = 1.32 \pm 1.31 \mu\text{S}$, $P < 0.01$), and for 2-to-3 ($\Delta = 1.76 \pm 1.68 \mu\text{S}$, $P < 0.01$) (Fig. 3B, Table I). SCR also significantly increased with increasing nausea level (from 0-to-1 to 2-to-3: $\Delta = 0.77 \pm 1.13 \mu\text{S}$, $P < 0.05$, and from 1-to-2 to 2-to-3: $\Delta = 0.44 \pm 0.67 \mu\text{S}$, $P < 0.05$) (Fig. 3B). HR significantly increased in all windows of interest (0-to-1: $\Delta = 8.4 \pm 7.0$ bpm, $P <$

TABLE I. SKIN CONDUCTANCE RESPONSE FROM BASELINE.

Stimulus-Based Analysis		
II	III	IV
0.68 \pm 0.98 μS (*)	1.94 \pm 1.65 μS (***)	2.46 \pm 2.11 μS (***)
Perception-Based Analysis		
"0-to-1"	"1-to-2"	"2-to-3"
0.99 \pm 1.26 μS (*)	1.32 \pm 1.31 μS (**)	1.76 \pm 1.68 μS (**)

Difference from baseline for both stimulus-based and perception-based analyses.

* = 0.01 < $P < 0.05$, ** = 0.001 < $P < 0.01$, *** = $P < 0.001$.

TABLE II. HEART RATE CHANGES FROM BASELINE.

Stimulus-Based Analysis		
II	III	IV
7.4 \pm 8.2 bpm (**)	12.0 \pm 7.0 bpm (***)	5.4 \pm 8.1 bpm (*)
Perception-Based Analysis		
"0-to-1"	"1-to-2"	"2-to-3"
8.4 \pm 7.0 bpm (***)	12.7 \pm 10.4 bpm (***)	15.0 \pm 11.4 bpm (***)

Difference from baseline for both stimulus-based and perception-based analyses.

* = 0.05 < $P < 0.1$, ** = 0.001 < $P < 0.01$, *** = $P < 0.001$.

0.001; 1-to-2: $\Delta = 12.7 \pm 10.4$ bpm, $P < 0.001$; 2-to-3: $\Delta = 15.0 \pm 11.4$ bpm, $P < 0.001$) (Fig. 3C, Table II). HR also significantly increased between 0-to-1 and 2-to-3 ($\Delta = 6.6 \pm 8.9$ bpm, $P < 0.05$) (Fig. 3C).

In regard to HRV, normalized HF significantly decreased from baseline following the 2-to-3 rating transition window ($\Delta = -0.11 \pm 0.13$ a.u., $P < 0.05$) (Fig. 3E), while normalized LF significantly increased following the 2-to-3 window ($\Delta = 0.13 \pm 0.16$ a.u., $P < 0.05$) (Fig. 3F). The LF/HF ratio also significantly increased over baseline following both the 1-to-2 transition ($\Delta = 1.54 \pm 2.11$ a.u., $P < 0.05$) and the 2-to-3 transition ($\Delta = 2.57 \pm 3.49$ a.u., $P < 0.05$) (Fig. 3G, Table III).

Point-process HF HRV data were analyzed for five 90-s temporal windows (START, 0-to-1, 1-to-2, 2-to-3, and END), averaged over all subjects (Fig. 4). For these group data, the "START" window demonstrated increasing HF, peaking 10 to 20 s after stimulus onset, with gradual decrease thereafter. Conversely, the "END" window demonstrated gradual increase in HF following stimulus cessation. The 0-to-1, 1-to-2, and 2-3 windows demonstrated gradual decrease in HF by 30 s after transition in nausea level, but interestingly, phasic bursts of HF increase were also seen 10 to 20 s before subjects rated a change in nausea level.

DISCUSSION

The autonomic outflow related to increasing nausea sensation following motion sickness is not fully understood. Our study employed a nauseogenic visual stimulus (horizontally translating stripes) while subjects freely rated transitions in their level of nausea and while we measured autonomic outflow to multiple end organs (heart, skin). Our design allowed us to relate ANS modulation with subject-specific nausea perception. Moreover, we adopted a recent (2,3) approach to continuous HRV estimation in order to evaluate dynamic cardiovagal response to increasing nausea perception. We found that nausea correlates with increased heart rate and skin conductance and has a more complex effect on measures of heart rate variability consistent with decreased cardiovagal modulation and a sympathetic shift in sympathovagal balance. Interestingly, our dynamic HRV measures demonstrated that bursts of cardiovagal modulation may accompany transitions in nausea perception level. Specifically, these bursts anticipate and may even play a role in promoting subjects to rate higher

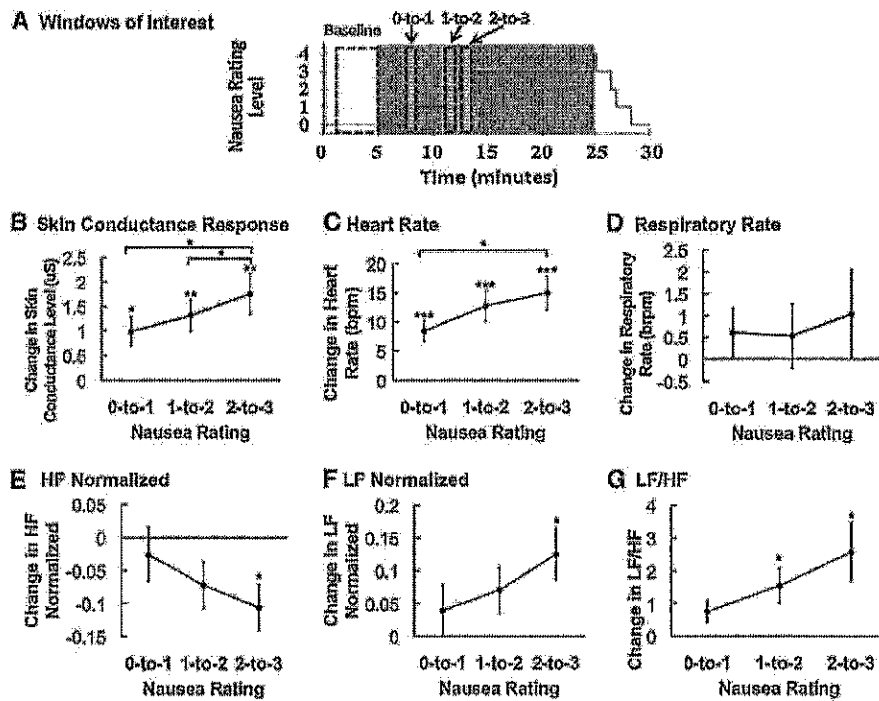


Fig. 3. Perception-based analysis of physiological indices. A) Timing of 4-min baseline and 1-min post-nausea rating transition windows are shown over a plot of a representative subject's nausea level. B-G) Mean change in SCL, HR, respiratory rate, normalized HF, normalized LF, and LF/HF ratio with increasing nausea level. Error bars indicate standard error of the mean. * 0.05 > P > 0.01, ** 0.01 > P > 0.001, *** P < 0.001.

levels of nausea. Our findings both corroborate several past autonomic studies of nausea, as well as apply, for the first time, dynamic tracking of cardiovagal modulation in response to increasing nausea perception.

Our study investigated nausea-related changes in HRV with both window-based (assumed stationary in time) and dynamic methods. In the first approach, which considered HF normalized, LF normalized, and LF/HF over the same intervals used for other physiological variables (HR, SCL), we found an overall decrease in HF normalized. This was coincident with an overall increase in LF normalized and, consequentially, an increase in LF to HF ratio during the presentation of the nauseogenic stimulus. These results are consistent with the tilting of sympathovagal balance away from cardiovagal modulation in response to increasing nausea intensity. We instructed subjects to not significantly alter their respiratory

rate to self-inhibit nausea and the lack of significant change in respiratory rate during the nauseogenic stimulation bolsters the interpretability of these HRV results (4,26).

Previous studies (13,21,30) also examined the effect of motion sickness-induced nausea on measures of HRV. However, these studies did not yield consistent findings. These inconsistencies may stem from differences in stimulus form (visual only versus both physical and visual) and intensity, differences in subject posture, or from methodological approaches to calculate HRV. Different nauseogenic stimuli (e.g., translating stripes versus rotating chairs) may lead to different intensities of motion sickness and induce different autonomic response patterns (6,10). In previous studies exploring HRV, only Kim et al. used visual stimulation without physical rotations or tilt and found, contrary to our results of decreased HF, an increase in a spectral metric analogous to HF HRV (21). However, the stimulus used by Kim et al. (naturalistic virtual reality game immersion) was likely much less nauseogenic than our stimulus (horizontally translating stripes), as we stimulated all subjects to "strong" nausea and most subjects all the way to "severe" nausea, on the verge of vomiting. In contrast, the study by Kim et al. included data from all subjects, only 79% of whom experienced any motion sickness (21). Thus, our stimulus was likely stronger and induced a more cardio-sympathetic tilt in sympathovagal balance, with decreased cardiovagal modulation. In addition, posture (e.g., standing versus seated versus supine) is also known to strongly influence HRV (26).

TABLE III. HEART RATE VARIABILITY CHANGES FROM BASELINE (LF/HF RATIO).

Stimulus-Based Analysis		
II	III	IV
-0.06 ± 0.98 a.u. (n.s.)	0.87 ± 1.57 a.u. (n.s.)	0.24 ± 0.96 a.u. (n.s.)
Perception-Based Analysis		
"0-to-1"	"1-to-2"	"2-to-3"
0.76 ± 1.36 a.u. (n.s.)	1.54 ± 2.11 a.u. (*)	2.57 ± 3.49 a.u. (*)

Difference from baseline for both stimulus-based and perception-based analyses.

* = 0.01 < P < 0.05, n.s. = not significant.

Specifically, in previous studies, subjects were seated, not lying supine as in our study. Finally, HRV is known to be strongly influenced by respiratory depth and rate (26). Thus, while our study did not find significant changes in respiration between nausea levels (we asked subjects to try to maintain constant respiration), other studies found significant increases (10,37) or decreases (21), which might have affected HRV results. Hence, interpretability of our results is improved and better supports the assertion that nausea is associated with decreased cardiovagal modulation and a sympathetic shift in sympathovagal balance.

We also applied a dynamic analysis approach, which used a previously validated point process algorithm to measure nonstationarities in HF over a much finer temporal window, to the HRV data. This approach revealed phasic bursts of HF that accompanied transitions in nausea level. Bursts can be seen just prior to rating increases to "1," "2," and "3." These cardiovagal bursts may be associated with the autonomic "flushes" that can accompany nausea and could then lead to interoceptive re-evaluation by the subject, culminating in the decision to rate a higher nausea intensity level. Such bursts may also be consistent with previous HRV studies for chemotherapy-induced nausea in patients, which demonstrated that the standard deviation of successive differences metric, a proxy for cardiovagal modulation, peaked just prior to nausea onset (29). In addition to these dynamic bursts, HF gradually decreased within a minute of nauseogenic stimulus initiation. Furthermore, within tens of seconds after nauseogenic stimulus cessation, HF gradually increased. This more gradual change may have reflected shifting anxiety levels in our subjects. Anxiety is known to influence both postoperative and chemotherapy-induced nausea (25,35) and motion sickness (36). In our study, anxiety likely increased as soon as the stimulus was presented (and before nausea

was actually induced). Also, anxiety was likely diminished once the nauseogenic stimulus stopped, as subjects learned from the previous training session that cessation of stimulus would soon lead to the cessation of the nausea sensation.

Skin conductance response increased both during nauseogenic stimulus presentation and with increasing nausea level, and continued increasing after cessation of stimulus. Other studies have found similar increases in skin conductance with increasing nausea stimulus duration (21). Also, the persistence of elevated skin conduction into the post-stimulus period has been previously documented (10,18). Skin conductance is purely controlled by the sympathetic nervous outflow to sudomotor glands in the skin (5,7,17) and persistence of elevated skin conduction may have been due to the known long latency characterizing this autonomic outflow system (7). Thus, our findings point to a highly persistent sympathetic outflow to the skin in response to nausea.

In contrast to skin conductance, which increased during nauseogenic stimulation and continued increasing after termination, we found that HR increased over the duration of stimulation and with increasing nausea level, only to drop off sharply after stimulus cessation. Increased HR is consistent with some studies which found HR increase in response to motion sickness (10,21,37), while other studies found no significant effect on heart rate (16,30). This seeming inconsistency may be due to differences in experimental and analysis procedures. Mullen et al. (30) averaged measurements over a very long period (15 min), during which subjects practiced random interval breathing, while Graybiel et al. (16) stopped stimulation periodically to take HR measurements, which may have affected the naturalistic context of progressively worsening motion sickness. For our study, the rapid decrease of heart rate immediately following nausea stimulus termination was also consistent with previous studies (10,21). As HR is influenced by both

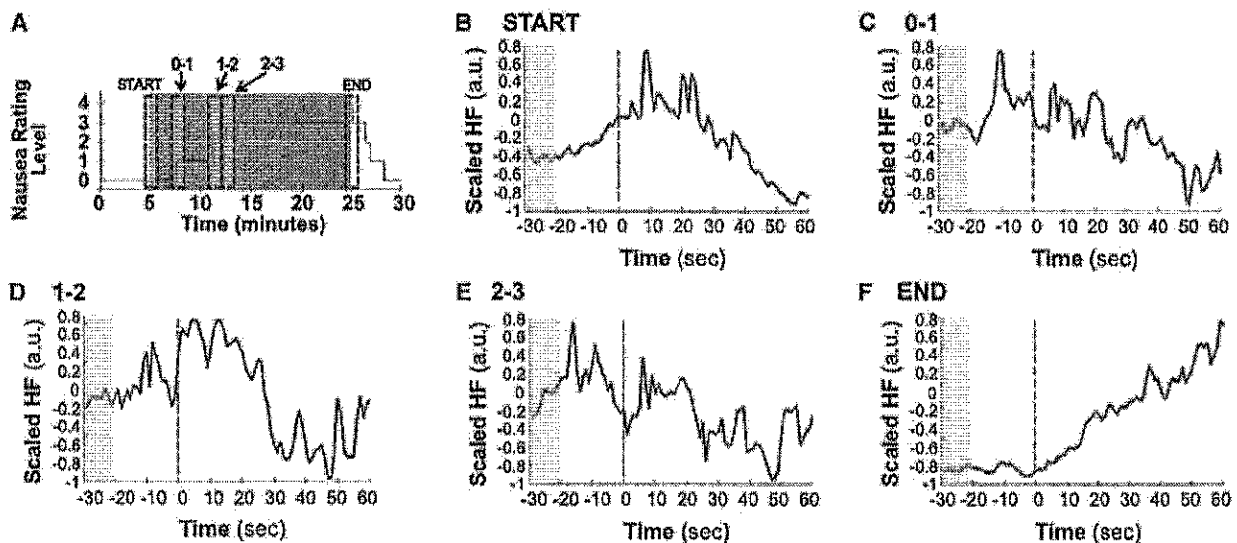


Fig. 4. Average across subjects of normalized point process HF HRV. A) Schematic representation of the 90-s window placements. B-F) HF HRV time series within windows of interest averaged across subjects following stimulus initiation through stimulus cessation.

the sympathetic and parasympathetic branch of the ANS, our findings may have resulted from either an increase in cardio-sympathetic modulation or a decrease in cardio-vagal modulation.

Several limitations to our study should be noted. First, some subjects (5 out of 17) did not reach a nausea level 4 within the 20 min maximally allotted for stimulation. For consistency, these five subjects were not used for analyses involving the stimulus termination landmark only. However, these five subjects demonstrated similar results to the main group for other temporal landmarks, so were likely not outliers and likely did not negatively skew the complete dataset. In addition, some subjects transitioned to higher nausea levels so quickly that there was minor overlap between test windows in our perception-related analysis. This happened for 2 (of 17) subjects and a subanalysis without these data did not change the final conclusions of our study. Another limitation was that our study population consisted entirely of female subjects due to limitations in recruitment. While gender appears to play only a minor role in motion sickness susceptibility (23), future studies should make a stronger effort to recruit male subjects. Finally, while a causal relationship is difficult to test with our approach, we have interpreted our findings to represent "nausea induced autonomic response," as windows of interest in the perception analysis followed transitions in nausea level. However, as suggested by the dynamic HRV results, some autonomic responses (e.g., bursting HF increase) may actually precipitate and ultimately induce increased nausea perception. This complex phenomenon should be investigated in future studies.

In conclusion, we found increases in both skin conductance and heart rate in response to increasing levels of nausea. We also found decreased HF HRV and increased LF HRV, resulting in an increasing LF/HF ratio with increasing nausea. A recently developed dynamic HF HRV measurement demonstrated that bursts of cardiovagal modulation may accompany (precede) transitions in perception level as subjects become more nauseous. Our findings suggest a robust ANS response to increasing nausea perception consistent with increased sympathetic and decreased parasympathetic modulation. Future studies should explore the neural correlates of this peripheral autonomic modulation.

ACKNOWLEDGMENTS

We would like to thank NIH for funding support (RB: R01-HL084502; EB: R01-DA015644 and DP1-OD003646; VN: K01-AT002166, P01-AT002048, R01-AT004714; KP: F05-AT003770; BK: K23-DK069614), the NCCR (P41RR14075; CRC 1 UL1 RR025758-01), the Mental Illness and Neuroscience Discovery (MIND) Institute, and the International Foundation of Functional GI Disorders. Dr. Park was also supported by the Institute of Information Technology Advancement, Korea IITA-2008-(C1090-0801-0002). We would also like to thank Dr. Mark Vangel for technical assistance on statistical analyses of the data.

Authors and affiliations: Lauren T. LaCount, B.S., Jicun Kim, Ph.D., and Vitaly Napadow, Ph.D., Martinos Center for Biomedical Imaging, Department of Radiology, Massachusetts General Hospital, Charlestown, MA; Riccardo Barbieri, Ph.D., and Emery N. Brown, M.D., Ph.D., Department of Anesthesia and Critical Care, Massachusetts General Hospital, Boston, MA; Kyungmo Park, Ph.D., Department of Biomedical Engineering, Kyunghee University, Yongin, Republic of Korea; and Braden Kuo, M.D., Gastroenterology Unit, Massachusetts General Hospital, Harvard Medical School, Boston, MA.

REFERENCES

- Anderson LA, Gross JB. Aromatherapy with peppermint, isopropyl alcohol, or placebo is equally effective in relieving postoperative nausea. *J Perianesth Nurs* 2004; 19:29-35.
- Barbieri R, Matten EC, Alabi AA, Brown EN. A point-process model of human heartbeat intervals: new definitions of heart rate and heart rate variability. *Am J Physiol Heart Circ Physiol* 2005; 288:H424-35.
- Barbieri R, Brown EN. Analysis of heartbeat dynamics by point process adaptive filtering. *IEEE Trans Biomed Eng* 2006; 53:4-12.
- Berntson GG, Bigger JT Jr, Eckberg DL, Grossman P, Kaufmann PG, et al. Heart rate variability: origins, methods, and interpretive caveats. *Psychophysiology* 1997; 34:623-48.
- Bini G, Hagbarth KE, Hynninen P, Wallin BG. Thermoregulatory and rhythm-generating mechanisms governing the sudomotor and vasoconstrictor outflow in human cutaneous nerves. *J Physiol* 1980; 306:537-52.
- Bos JE, Bles W. Motion sickness induced by optokinetic drums. *Aviat Space Environ Med* 2004; 75:172-4.
- Boucsein W. *Electrodermal activity*. New York: Plenum Press; 1992.
- Bubka A, Bonato F. Optokinetic drum tilt hastens the onset of vection-induced motion sickness. *Aviat Space Environ Med* 2003; 74:315-9.
- Cheung BS, Howard IP, Money KE. Visually induced sickness in normal and bilaterally labyrinthine-defective subjects. *Aviat Space Environ Med* 1991; 62:527-31.
- Cowings PS, Suter S, Toscano WB, Kamiya J, Naifeh K. General autonomic components of motion sickness. *Psychophysiology* 1986; 23:542-51.
- Cowings PS, Naifeh KH, Toscano WB. The stability of individual patterns of autonomic responses to motion sickness stimulation. *Aviat Space Environ Med* 1990; 61:399-405.
- Denise P, Vouriot A, Normand H, Golding JE, Gresty MA. Effect of temporal relationship between respiration and body motion on motion sickness. *Auton Neurosci* 2009; 151:142-6.
- Doweck I, Gordon CR, Shlittner A, Spitzer O, Gonen A, et al. Alterations in R-R variability associated with experimental motion sickness. *J Auton Nerv Syst* 1997; 67:31-7.
- Goldberger AL, Amaral LA, Glass L, Hausdorff JM, Ivanov PC, et al. *PhysioBank, PhysioToolkit, and PhysioNet: components of a new research resource for complex physiologic signals*. *Circulation* 2000; 101:E215-20.
- Golding JE. Motion sickness susceptibility questionnaire revised and its relationship to other forms of sickness. *Brain Res Bull* 1998; 47:507-16.
- Graybiel A, Lackner JR. Evaluation of the relationship between motion sickness symptomatology and blood pressure, heart rate, and body temperature. *Aviat Space Environ Med* 1980; 51:211-4.
- Harm DL. Motion sickness neurophysiology, physiological correlates, and treatment. In: Stanney KM, ed. *Handbook of virtual environments*. Mahwah, NJ: Lawrence Erlbaum Associates; 2002:637-61.
- Isu N, Koo J, Takahashi N. Changes of skin potential level and of skin resistance level corresponding to lasting motion discomfort. *Aviat Space Environ Med* 1987; 58:136-42.
- Kennedy RS, Lane NE, Berbaum KS, Lillenthal MG. Simulator Sickness Questionnaire: an enhanced method for quantifying simulator sickness. *Int J Aviat Psychol* 1993; 3:203-30.
- Kennedy RS, Drexler J, Kennedy RC. Research in visually induced motion sickness. *Appl Ergon* 2010; 41:494-503.
- Kim YY, Kim HJ, Kim EN, Ko HD, Kim HT. Characteristic changes in the physiological components of cybersickness. *Psychophysiology* 2005; 42:616-25.
- Klosterhalfen S, Kellermann S, Pan F, Stockhorst U, Hall G, Enck P. Effects of ethnicity and gender on motion sickness susceptibility. *Aviat Space Environ Med* 2005; 76:1051-7.
- Klosterhalfen S, Pan F, Kellermann S, Enck P. Gender and race as determinants of nausea induced by circular vection. *Genet Med* 2006; 3:236-42.
- Koch KL. Illusory self-motion and motion sickness: a model for brain-gut interactions and nausea. *Dig Dis Sci* 1999; 44(8, Suppl.):53S-7S.

AUTONOMIC RESPONSE TO NAUSEA—LACOUNT ET AL.

25. Lee YY, Kim KH, Yom YH. Predictive models for post-operative nausea and vomiting in patients using patient-controlled analgesia. *J Int Med Res* 2007; 35:497–507.
26. Task Force of the European Society of Cardiology and the North American Society of Pacing and Electrophysiology. Heart rate variability. Standards of measurement, physiological interpretation, and clinical use. *Eur Heart J* 1996; 17:354–81.
27. Task Force of the European Society of Cardiology. Heart rate variability: standards of measurement, physiological interpretation and clinical use. *Circulation* 1996; 93:1043–65.
28. Miller JC, Sharkey TJ, Graham GA, McCauley ME. Autonomic physiological data associated with simulator discomfort. *Aviat Space Environ Med* 1993; 64:813–9.
29. Morrow GR, Andrews PL, Hickok JT, Stern R. Vagal changes following cancer chemotherapy: implications for the development of nausea. *Psychophysiology* 2000; 37:378–84.
30. Mullen TJ, Berger RD, Oman CM, Cohen RJ. Human heart rate variability relation is unchanged during motion sickness. *J Vestib Res* 1998; 8:95–105.
31. Muth ER. Motion and space sickness: intestinal and autonomic correlates. *Auton Neurosci* 2006; 129:58–66.
32. Napadow V, Dhond R, Conti G, Makris N, Brown EN, Barbieri R. Brain correlates of autonomic modulation: combining heart rate variability with fMRI. *Neuroimage* 2008; 42:169–77.
33. Oldfield RC. The assessment and analysis of handedness: the Edinburgh inventory. *Neuropsychologia* 1971; 9:97–113.
34. Parker DE. The relative roles of the otolith organs and semicircular canals in producing space motion sickness. *J Vestib Res* 1998; 8:57–9.
35. Shih V, Wan HS, Chan A. Clinical predictors of chemotherapy-induced nausea and vomiting in breast cancer patients receiving adjuvant doxorubicin and cyclophosphamide. *Ann Pharmacother* 2009; 43:444–52.
36. Stern RM, Koch KL. Motion sickness and differential susceptibility. *Curr Dir Psychol Sci* 1996; 5:115–20.
37. Stout CS, Toscano WB, Cowings PS. Reliability of psychophysiological responses across multiple motion sickness stimulation tests. *J Vestib Res* 1995; 5:25–33.
38. Wiggins GC, Triantafyllou C, Potthast A, Reykowski A, Nittka M, Wald LL. 32-channel 3 Tesla receive-only phased-array head coil with soccer-ball element geometry. *Magn Reson Med* 2006; 56:216–23.

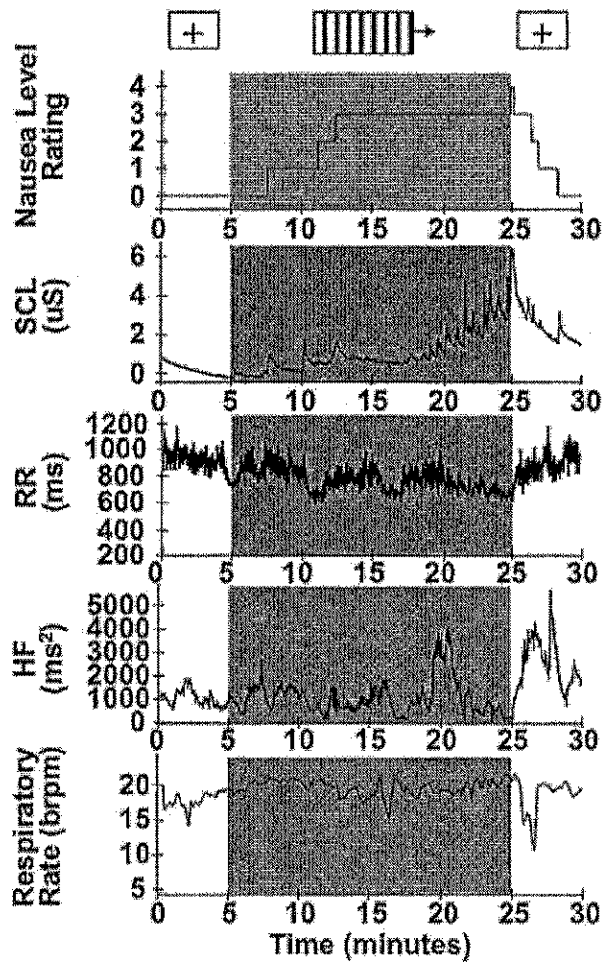


Fig. A. Nausea level, SCL, HR, HF HRV, and respiratory rate for one representative subject over the course of the experiment. The gray region of each plot indicates when the nauseogenic visual stimulus was on, whereas the remaining white regions indicate when subjects were simply visually fixating (also indicated by stripes and cross hair at top of figure, respectively).